

# Experimental Procedure Designed to Determine the Elastic Characteristics of Fiber-Reinforced Polymeric Composite Materials

VIORIEL GOANTA<sup>1\*</sup>, ANTON HADAR<sup>2</sup>, BOGDAN LEITOIU<sup>1</sup>

<sup>1</sup> Technical University "Gh. Asachi" Iași, Department of Strength of Materials, Bd. Mangeron, 700050, Romania

<sup>2</sup> University Politehnica of Bucharest, Department of Strength of Materials, 313 Splaiul Independentei, 060042, Bucharest, Romania

*Fiber-reinforced polymeric composite materials present an orthotropic distribution of their mechanical and elastic characteristics. This behaviour is mainly due to the fact that the fabric used behaves differently under the same type of stress, on different directions. The procedure described by our paper enables researchers to determine the elastic modulus of such materials, on three different directions, using a specially designed specimen. The finite element analysis revealed that there were no significant influences on the strains and deformations existing in the measurement area, concerning the shape of the test specimen or its fastening. The results obtained for three composite materials used to validate the procedure showed that two of the materials having orthotropic properties, exhibit different elastic modulus.*

*Keywords: polymeric composite, deformations, octagonal specimen, orthotropy, elastic characteristics*

The mechanical and elastic characteristics of a composite material are strongly influenced by the properties and distribution of its constituents, as well as by the interactions among them. In addition to the nature and properties of its constituents, the analysis of a composite material considered as a system should also refer to the geometry of the reinforcement in the whole system, which geometry may be defined by shape, size, proportions and distribution. Homogeneity is an important characteristic that determines the extent to which a large portion of material may differ from the viewpoint of its physical, mechanical and elastic properties, as compared to the average properties of the material. System unevenness should be prevented, as it dictates the properties governed by the poorest bonds in the material.

Reinforcement orientation affects system isotropy. Let us consider a piece of homogeneous, elastic and isotropic material in which we cut up four test specimens having similar sizes in order to subject them to tensile strength tests [1] (fig. 1a). If we resort to a graphic representation of the variations of the normal strain values  $\sigma$  compared with the specific elongations  $\epsilon$ , we notice that the diagrams of the four test specimens are identical or almost identical, figure 1b. If the material of the test specimens is isotropic, the curve identity deviation is blamed on the imperfections of the testing method: test specimens with size deviations,

wrong specimen fastening in the testing equipment, reading errors, etc. For a homogeneous and isotropic material, the strain-deformation ratio depends neither on the point nor on the direction of the measurement. The elastic characteristics of such a material are expressed by two constants: the E longitudinal modulus of elasticity, or Young's modulus, and the contraction of transverse strain  $\nu$ , or Poisson's ratio.

If tensile strength tests are performed on test specimens on the same x and y directions of a unidirectional reinforcement composite material (fibers on the y direction, for instance), we notice that the diagrams of the 1 and 1' test specimens are also identical, as the material is homogeneous (fig. 1c). On the other hand, the diagrams of the 1 and 2 test specimens, cut up on the y and x directions, respectively, are completely different (fig. 1c). The yield strength does not have the same value in this last case, and Young's modulus and Poisson's ratio are also different. This material is defined as homogeneous and anisotropic. Its mechanical and elastic properties do not depend on the point they refer to, but on the direction of the tensile strength.

In order to characterize the behaviour of such materials, that is in order to define the relation between strains and specific deformations, one should generally know and therefore determine 36 elastic modulus.

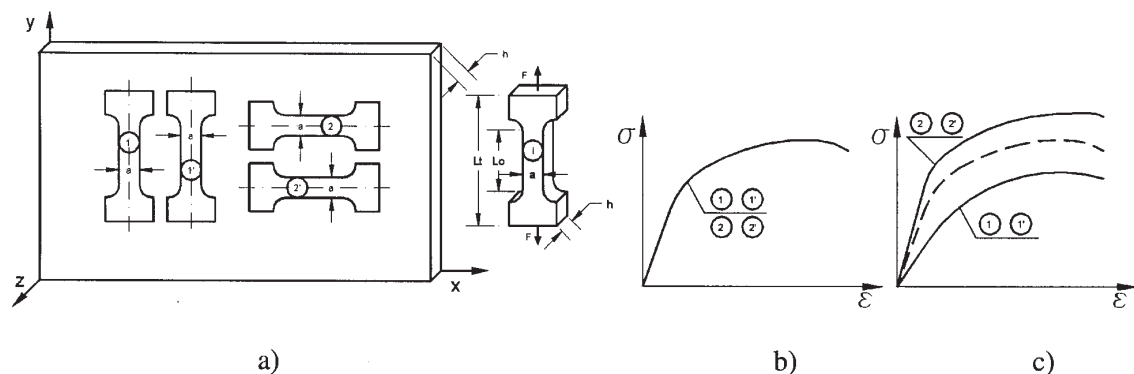


Fig. 1. Test specimen cutting up for the determination of the elastic characteristics

\* Tel.: 0232278688

### Constituent Relations of the Elasticity of an Anisotropic Material

Constituent or physical equations between strains and deformations may be generally expressed as a matrix [1]:

$$\begin{Bmatrix} \varepsilon_{xx} \\ \varepsilon_{yy} \\ \varepsilon_{zz} \\ \varepsilon_{yz} \\ \varepsilon_{xz} \\ \varepsilon_{xy} \end{Bmatrix} = \begin{bmatrix} \bar{S}_{11} & \bar{S}_{12} & \bar{S}_{13} & \bar{S}_{14} & \bar{S}_{15} & \bar{S}_{16} \\ \bar{S}_{21} & \bar{S}_{22} & \bar{S}_{23} & \bar{S}_{24} & \bar{S}_{25} & \bar{S}_{26} \\ \bar{S}_{31} & \bar{S}_{32} & \bar{S}_{33} & \bar{S}_{34} & \bar{S}_{35} & \bar{S}_{36} \\ \bar{S}_{41} & \bar{S}_{42} & \bar{S}_{43} & \bar{S}_{44} & \bar{S}_{45} & \bar{S}_{46} \\ \bar{S}_{51} & \bar{S}_{52} & \bar{S}_{53} & \bar{S}_{54} & \bar{S}_{55} & \bar{S}_{56} \\ \bar{S}_{61} & \bar{S}_{62} & \bar{S}_{63} & \bar{S}_{64} & \bar{S}_{65} & \bar{S}_{66} \end{bmatrix} \begin{Bmatrix} \sigma_{xx} \\ \sigma_{yy} \\ \sigma_{zz} \\ \sigma_{yz} \\ \sigma_{xz} \\ \sigma_{xy} \end{Bmatrix} \quad (1)$$

The ratio (1) may be written as follows:

$$\{\varepsilon_{ij}\} = [\bar{S}_{ij}] \cdot \{\sigma_{ij}\} \quad (2)$$

where:

- $\{\varepsilon_{ij}\}$  are the components of the deformation tensor for the spatial stress-strain state;
- $\{\sigma_{ij}\}$  are the components of the strain tensor for the spatial stress-strain state;
- $[\bar{S}_{ij}]$  is called compliance or elasticity matrix.

The  $[\bar{S}_{ij}]$  terms are represented by the elastic characteristics of the material.

Orthotropy is a particular case of anisotropy. Materials having orthotropic characteristics has 3 elastic characteristic symmetry planes, figure 2.

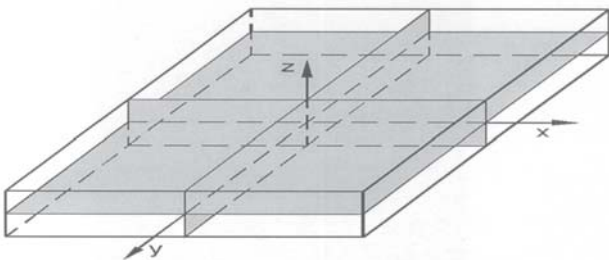


Fig. 2. Orthotropic material: symmetry planes and main directions

In case of stresses applied to the main material directions, the constituent relations are mostly known under the name of Hooke's law in space and they may also be described by the following matrix:

$$\begin{Bmatrix} \varepsilon_{xx} \\ \varepsilon_{yy} \\ \varepsilon_{zz} \\ \varepsilon_{yz} \\ \varepsilon_{xz} \\ \varepsilon_{xy} \end{Bmatrix} = \begin{bmatrix} S_{11} & S_{12} & S_{13} & 0 & 0 & 0 \\ S_{21} & S_{22} & S_{23} & 0 & 0 & 0 \\ S_{31} & S_{32} & S_{33} & 0 & 0 & 0 \\ 0 & 0 & 0 & S_{44} & 0 & 0 \\ 0 & 0 & 0 & 0 & S_{55} & 0 \\ 0 & 0 & 0 & 0 & 0 & S_{66} \end{bmatrix} \begin{Bmatrix} \sigma_{xx} \\ \sigma_{yy} \\ \sigma_{zz} \\ \sigma_{yz} \\ \sigma_{xz} \\ \sigma_{xy} \end{Bmatrix} \quad (3)$$

where:

$$\text{where: } S_{11} = \frac{1}{E_{11}}; S_{12} = S_{21} = -\frac{\nu_{12}}{E_{11}} = -\frac{\nu_{21}}{E_{22}}; S_{13} = S_{31} = -\frac{\nu_{13}}{E_{11}} = -\frac{\nu_{31}}{E_{33}};$$

$$S_{22} = \frac{1}{E_{22}}; S_{23} = S_{32} = -\frac{\nu_{23}}{E_{22}} = -\frac{\nu_{32}}{E_{33}}; S_{33} = \frac{1}{E_{33}}; S_{44} = \frac{1}{G_{23}}; S_{55} = \frac{1}{G_{31}}; S_{66} = \frac{1}{G_{12}} \quad (4)$$

The elasticity of the orthotropic material is defined by 9 independent elastic characteristics, as shown in ratio (4). Considering that the transverse elasticity modulus (Coulomb)  $G_{ij}$  of some materials may be calculated according to the following ratio:

$$G = \frac{E}{2(1+\nu)} \quad (5)$$

in order to define the elastic characteristics of an orthotropic body, we need 3 Young's modulus, that is  $E_{11}$ ,  $E_{22}$  and  $E_{33}$ , and three Poisson's ratios, that is  $\nu_{12}$ ,  $\nu_{13}$  and  $\nu_{23}$ . We suggest nonetheless that the Coulomb's modulus values be determined on Iosipescu test specimens, cut up separately and oriented on the directions described herein.

### Elastic Modulus Determination using Electrical Resistance Tensometry

In strength of materials, deformation and stability calculations, in experimental strain analysis and in finite element analysis, knowing the elastic characteristics of the materials that the constituent pieces or items are made of are absolutely necessary [2-4]. For the experimental analysis of the strains occurring in the fiber-reinforced polymeric matrix composite materials, it is wiser to rely on the material mechanical and elastic characteristics as determined by the user and not on the values calculated in literature. From the viewpoint of the fiber reinforcement method employed, these materials may be considered orthotropic. There are several methods employed to determine the elastic characteristics of these types of materials, some of which involve the use of electrical resistance tensometry. This method determines the elastic characteristics of test specimens subject to tensile strength testing, according to ASTM D3039. In order to determine the 6 elastic characteristics described above, we need three sets of test specimens cut up on the x, y and z directions, as shown in figure 2. If the piece of material is thin, the test specimens cannot be cut up on the z direction. For this same piece of material, we need to determine its elastic characteristics on a direction forming an up to 45° angle with, for instance, the longitudinal fibers [5]. If this is the case, a new set of test specimens should be cut up, in order to be able to determine their elastic characteristics.

This paper describes an experimental procedure able to determine, on a single specially designed test specimen (fig. 2) the elastic characteristics of a fiber-reinforced composite material on three directions belonging to the same plane.

Electrical resistance tensometry allows high accuracy specific, longitudinal and transverse deformation measurements. In order to determine specific deformations, on a flat tensile strength test specimen with a cross-section area of  $S_0 = (a \cdot b)$ , we fasten bidirectional electrical-tensometric rosettes (fig. 3). A grid of the TER1 rosette, that is ( $m_1$ ), is guided on the first direction, while the other, that is ( $m_3$ ), is guided on the third perpendicular direction. On the opposite side of the test specimen, in the middle of it, another bidirectional rosette (TER2) is

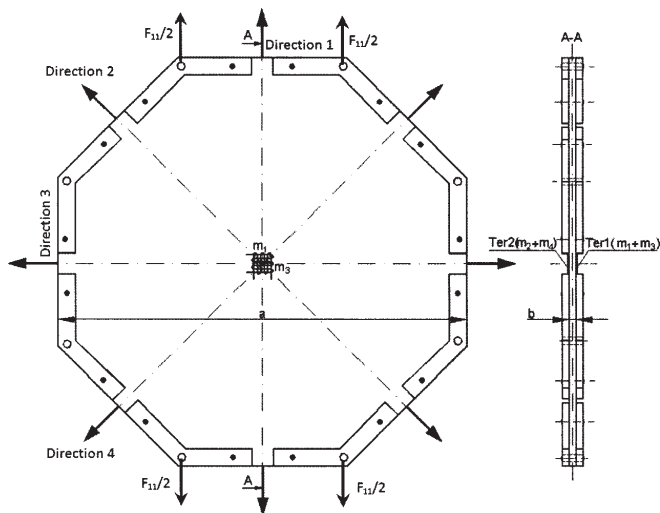


Fig. 3. Special tensile strength test specimen; tensometric transducer location



Fig. 4. Tensile strength testing of octagonal specimens

fastened, while its grids are laid out on the second, ( $m_2$ ), and fourth, ( $m_4$ ), directions, respectively. Therefore, stresses applied on the first direction result in the  $E_{11}$  and  $\nu_{13}$  elastic modulus, stresses applied on the second direction reveal the  $E_{22}$  and  $\nu_{24}$  elastic modulus, while stresses applied on the third direction result in the  $E_{33}$  and  $\nu_{31}$  elastic modulus.

Electrical-tensometric transducers are introduced in Wheatstone bridge measuring circuits with quarters of bridge configurations, which means that each tensometric mark is balanced according to the circuit in the tensometric bridge. By using the test specimen shown in figure 3, we may determine the  $E$  and  $\nu$  elastic characteristics on the first, second and third directions shown in the figure. If we use a test specimen having a similar shape with that shown in figure 3, it is no longer necessary to cut up three different test specimens on the longitudinal first, second and third directions. On the other hand, when using only this specimen, we are able to determine only the elastic characteristics occurring in the middle of the test specimen, while by cutting up different test specimens, we are able to determine the same characteristics in different points. In this case, however, errors may occur due to possible material imperfections in different areas caused either by the matrix or the reinforcement, or by the matrix and reinforcement interface.

### Experimental part

In order to calculate Young's modulus and Poisson's ratios on the first and third directions, the  $m_1$  and  $m_3$  tensometric marks will play, in turns, the role of

longitudinal and transverse marks. Therefore, for a better data systematization, the following specifications should be made:

- the  $m_1$ ,  $m_2$ ,  $m_3$  and  $m_4$  marks are displayed longitudinally, on proper directions;
- when the stress is applied on the first direction, upon signal reception, the  $m_1$  mark becomes the  $m_{1L}$  mark, and the  $m_3$  mark becomes the  $m_{3T}$  mark;
- when the stress is applied on the third direction, the  $m_1$  mark becomes the  $m_{1T}$  mark, while the  $m_3$  mark becomes the  $m_{3L}$  mark;
- when the stress is applied on the second direction, the  $m_2$  mark becomes the  $m_{2L}$  mark, and the  $m_4$  mark becomes the  $m_{4T}$  mark;

The tensile strength test on the specimens in figure 4 was performed using a universal tensile strength Instron 8801 testing system (fig. 4).

The software of this testing equipment records the data on all the tests performed on it. Thus, we have access to a data file including, among others, tensile strength variation with time. The tensometric mark signals were gathered using a Vishay P3 bridge. Strength control was applied to the testing system, while the test was performed at a 0.05 kN/min speed. At the same time, considering that the minimum data collection sampling rate for the Vishay bridge is 1 second, we set a similar data collection rate on the Instron testing system.

For this experiment we used the 3 types of specimens shown in figure 5, namely:

- a 0.9 mm thick specimen with epoxy resin matrix reinforced with a single layer of fiber glass;

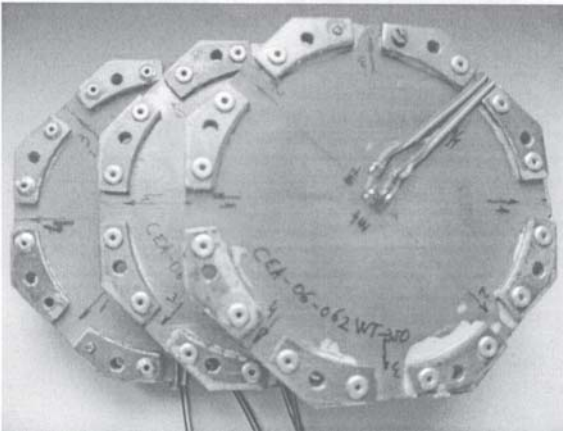


Fig. 5. Octagonal specimens submitted to tensile strength testing

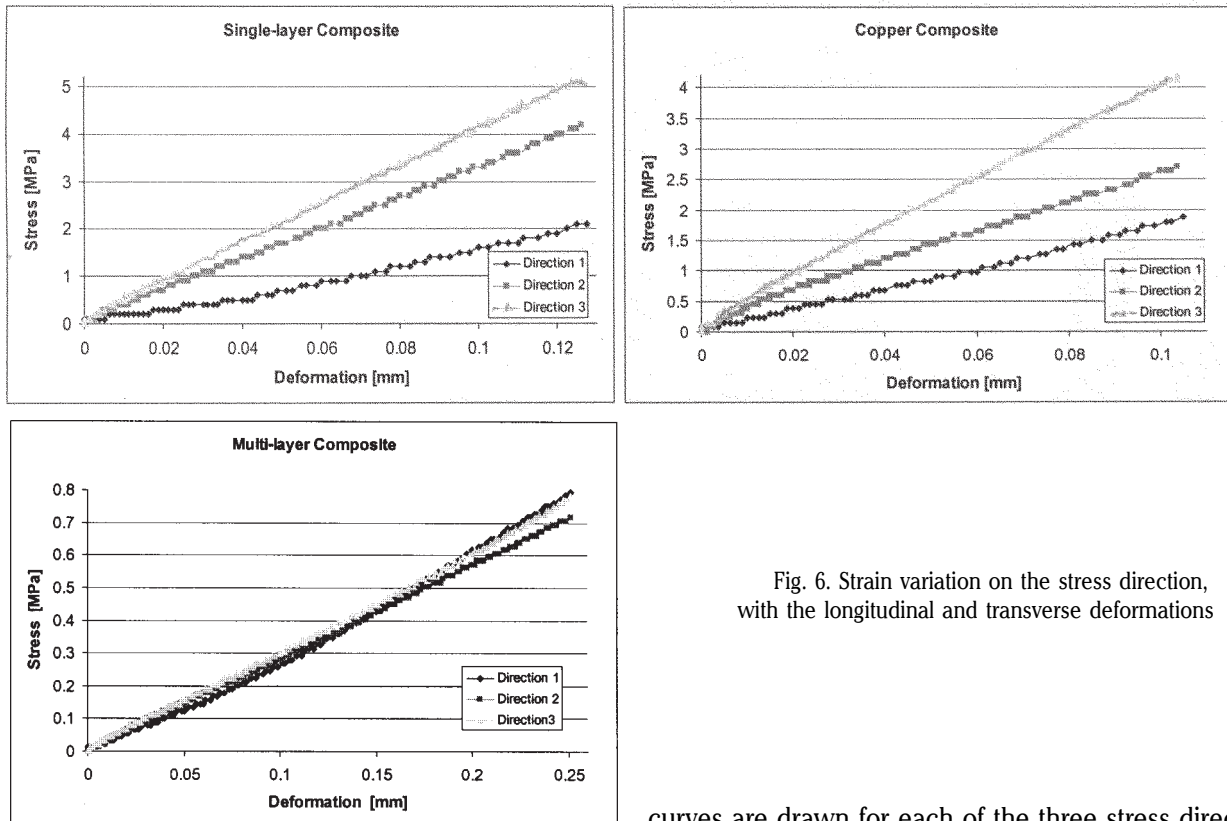


Fig. 6. Strain variation on the stress direction, with the longitudinal and transverse deformations

- a 1.2 mm thick specimen with epoxy resin matrix reinforced with a single layer of fiber glass and also copper coated;

- a 10 mm thick specimen with epoxy resin matrix reinforced with several layers of fiber glass.

The configuration of the specimens in figure 5 is the result of the need to achieve stresses on three directions: 0, 45 and 90°, as well as to allow their die clamping (fig. 4).

The testing system software provides a data file including strength and/or strain variation with time. By means of automatic data collection on the tensometric Vishay bridge, the latter memory card records the data file containing specific longitudinal and transverse deformation variation with time, when the specimen stress is applied on a particular direction.

If we remove the time factor from the two data files, we obtain a single file including stress strength (strain) variation with specific longitudinal and transverse deformations. The number of measurement points is relatively high further to the settings performed for the testing speed and the maximum elastic strength applied to the specimen. Figure 6 shows the strain variation curves on the stress direction, with the longitudinal and transverse deformations. These

curves are drawn for each of the three stress directions shown in figure 3.

For the first two specimens, which have a single fiber glass reinforcement layer, the first direction is the warp direction, the third direction is the weft direction, while the second direction forms a 45° angle with any of the two directions described above. The third specimen is a multi-layer composite, in which the warp directions in two successive layers are mutually perpendicular.

Here is the actual performance of the tests.

The piece of composite material is subject to tensile strength tests on the  $j$  (1, 2, and 3) directions. The piece of material also undergoes static charging at low speed and testing machine strength control. For the stresses applied on each direction, the tensometric Vishay bridge records the signals received from the  $m_1$ ,  $m_2$ ,  $m_3$  and  $m_4$  tensometric marks. Thus, when stresses are applied on the first direction, using  $F_{11}$  strengths, the  $m_1$  and  $m_3$  marks send out the  $m_{1L}$  signal, which represents the specific  $\epsilon_{1L}$  elongation, as well as the  $m_{3T}$  signal, standing for the specific transverse  $\epsilon_{3T}$  deformation, by means of which we are able to determine the  $E_{11}$  longitudinal elasticity modulus and  $\nu_{13}$  Poisson's ratio. Upon stress application on the second direction, using  $F_{21}$  strengths, the  $m_2$  and  $m_4$  marks send out the  $m_{2L}$

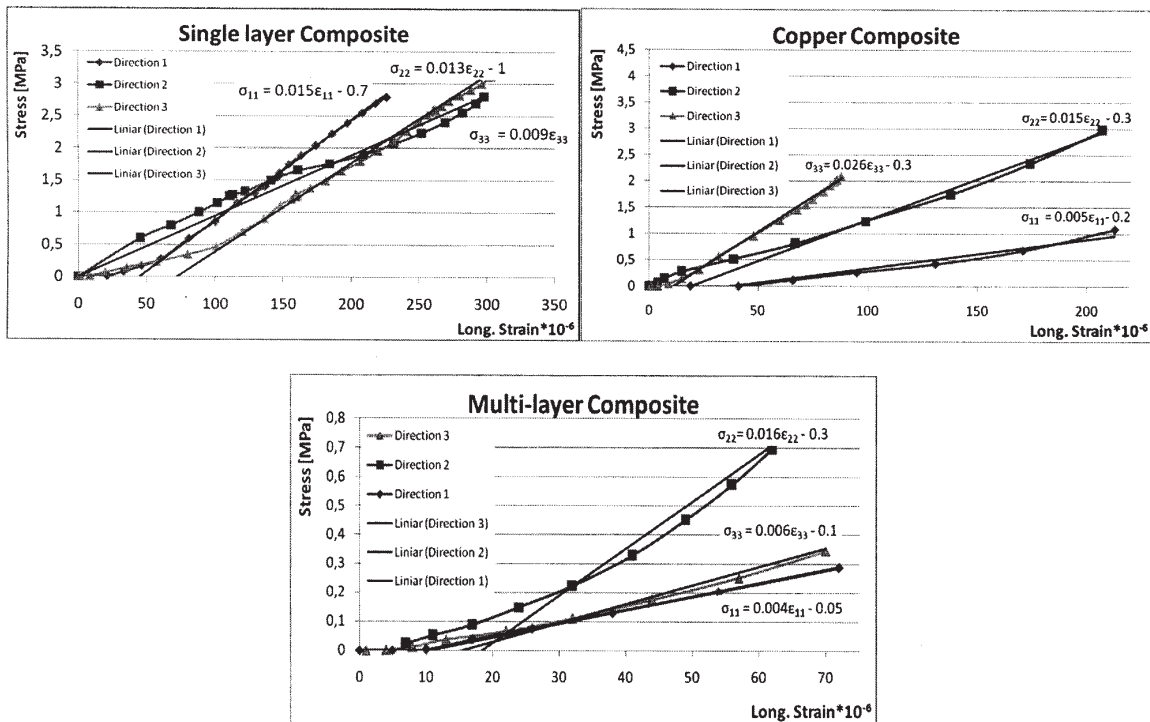


Fig. 7. Strain variation with longitudinal deformation – approximation lines for longitudinal elasticity modulus determination

signal, that is the specific  $\epsilon_{2L}$  elongation, as well as the  $m_{4T}$  signal representing specific transverse  $\epsilon_{4T}$  deformation, by means of which we are able to determine the  $E_{22}$  longitudinal elasticity modulus and  $\nu_{24}$  Poisson's ratio. Finally, when stresses are applied on the third direction, using  $F_{3i}$  strengths, the  $m_3$  and  $m_1$  marks send out the  $m_{3L}$  signal, which represents the specific  $\epsilon_{3L}$  elongation, as well as the  $m_{1T}$  signal, standing for the specific transverse  $\epsilon_{1T}$  deformation, by means of which we are able to determine the  $E_{33}$  longitudinal elasticity modulus and  $\nu_{31}$  Poisson's ratio.

### Results and discussions

According to figure 7, single fiber layer specimens reveal significant differences as concerns the strain-deformation diagrams drawn and the related values, which were determined for the three stress directions described above. On the other hand, the multi-layer composite specimen shows similar curves for the three directions above. If we consider however the fact that the beginning of the tests is obviously influenced by the manner in which the specimens are displayed in the device used for tensile strength application, we should remove the first data corresponding to the non-linear portion of the curves in figure 6. The data are processed in order to calculate the values of the elastic modulus of the composite materials on the first, second and third directions, as shown in figure 3:

- the  $E$  longitudinal elasticity modulus (Young's modulus) is determined as the gradient of the approximation line of the graph, formed by the normal strain ( $\sigma$ )/specific longitudinal deformation ( $\epsilon$ ) coordinates, through the points determined by the signals sent out by the longitudinal transducers;

- the  $\nu$  contraction of transverse strain (Poisson's ratio) is determined by the curve formed by the specific transverse deformation ( $\epsilon_{tr}$ )/specific longitudinal deformation ( $\epsilon_{long}$ ) coordinates, using signals obtained from both longitudinal and transverse traducers;

- the  $G$  transverse elasticity modulus (Coulomb) is calculated using the  $E$  and  $\nu$  constants, according to the ratio (5).

The test specimen cross-section is shown by the  $S_0 = a \cdot b$  [mm<sup>2</sup>] ratio, with the  $a$  and  $b$  sizes measured as shown in figure 3. If we consider the strength values recorded during the tests, strain is calculated from the data file, using the ratio:  $\sigma_i = F/S_0$  [N/mm<sup>2</sup>]. For the loading of each  $j$  stress direction, we draw the strain variation lines with specific  $\epsilon_L$  elongation, as we previously discussed (fig. 7). For these curves, we draw an approximation line that is almost tangent to the last portion of those curves. Thus, the gradients of the lines in figure 7 represent the  $E_{ij}$  elasticity modulus of the composite material on the three stress directions. The  $E_{ij}$  value for a specific direction is automatically revealed as the  $\epsilon_{ij}$  term coefficient of the ratios in the graphs in figure 7. In order to calculate the longitudinal elasticity modulus in N/mm<sup>2</sup>, that value must be multiplied by 10<sup>6</sup>.

The contraction of transverse strain (Poisson) is the proportionality factor between the transverse  $\epsilon_T$  deformation and the  $\epsilon_L$  longitudinal deformation, which also being the gradient of the line drawn in the ( $\epsilon_T$ ,  $\epsilon_L$ ) coordinates:

$$\epsilon_T = -\nu \cdot \epsilon_L \quad (6)$$

Specific transverse  $\epsilon_T$  deformation is measured using the  $m_3$ ,  $m_4$  and  $m_1$  tensometric marks (fig. 3), when the stress is applied on the first, second and third directions. These marks send out the signals of the specific transverse  $\epsilon_{3T}$ ,  $\epsilon_{4T}$  and  $\epsilon_{1T}$  deformations. These, together with the specific  $\epsilon_{1L}$ ,  $\epsilon_{2L}$  and  $\epsilon_{3L}$  elongations, form the graphs in figure 8. For these curves, we draw an approximation line that is almost tangent to the last portion of those curves.

Thus, the gradients of the lines already drawn are the contraction of transverse strain coefficients (Poisson's ratio) of the composite  $\nu_{jk}$  material, on the three stress directions. With  $E_{ij}$  and  $\nu_{jk}$  thus determined, the calculation

of the transverse elasticity  $G_{ij}$  modulus is possible for the three stress directions:

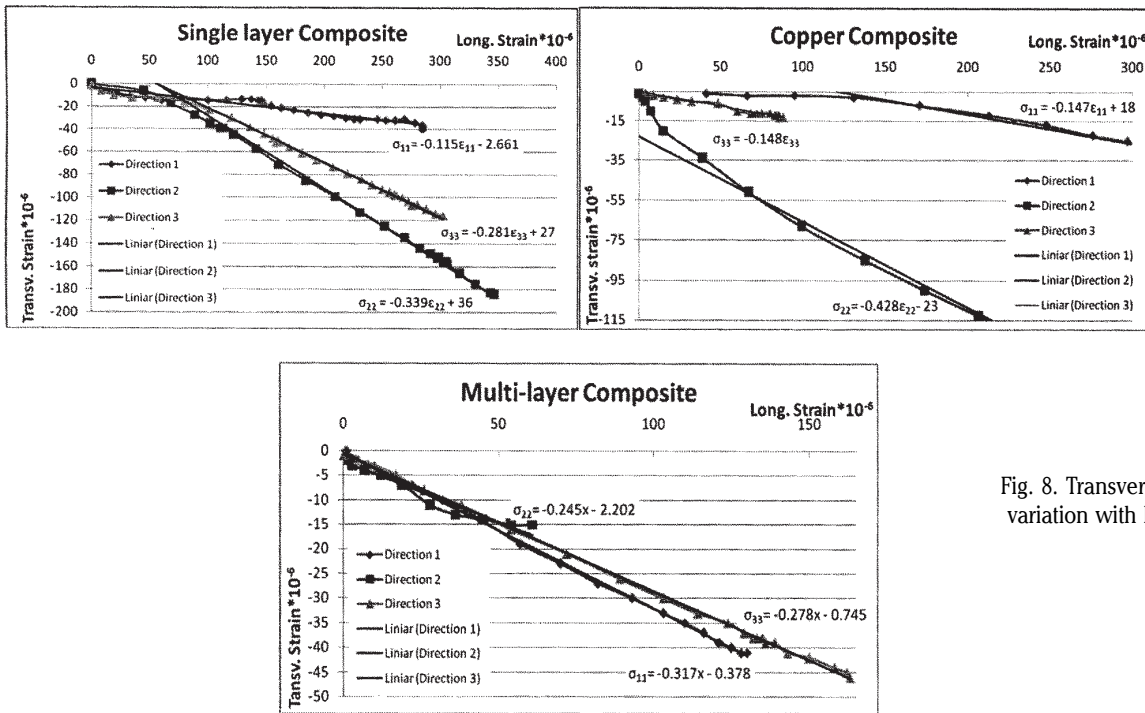


Fig. 8. Transverse deformation variation with longitudinal

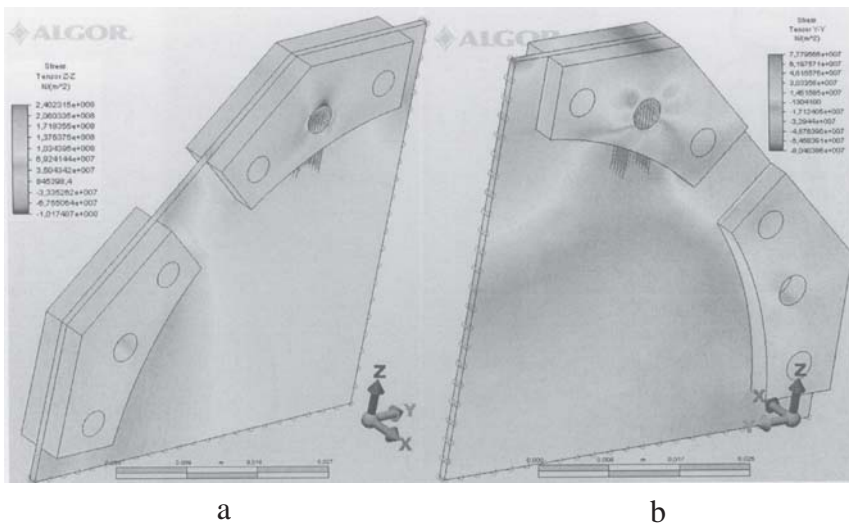


Fig. 9. Maps of  $\sigma$  strains on the z-z stress direction a) and on the y-y direction, perpendicular to strain b)

### Finite Element Analysis

In order to determine the influence of test specimen fastening in the testing device, we carried out a finite element analysis, figure 9. Please note that the finite element analysis was performed on the specimen containing the fastening elements shown in figure 5. The analysis was conducted on a model representing a quarter of the real test specimen, with the observance of the limiting conditions imposed by symmetry:

- the elements on the Y axis were prevented from undergoing Z axis translation and X and Y axes rotations;
- the elements on the Z axis were prevented from undergoing Y axis translation and X and Z axes rotations.

Figure 9 shows the strains in the central piece of material subject to mono-axial tensile strength testing, as shown in figure 3. Figure 9a shows the strain map on the z-z strain direction, while figure 9b shows the strain map on the y-y direction, which is perpendicular to the stress direction. The two figures show that the strains in the middle of the test specimen, where the electrical-tensometric transducers are located, are not influenced by the strain

concentrators. Consequently, considering both the configuration of the specimen and its fastening elements, the measurements performed by the tensometric marks located in the middle of the test specimen are not influenced.

### Conclusions

The value of the elastic characteristics of fiber-reinforced polymeric composite materials is important for resistance, deformation and stability calculations, for experimental strain analysis and for finite element analysis. These materials enjoy an orthotropic distribution of their elastic characteristics. Therefore, the procedure described in our paper allows elastic characteristic determination using a single test specimen. The test specimen is octagonal and has two electrical-tensometric transducers applied in the middle, on both sides, which transducers include two superimposed mutually perpendicular marks. This tensometric mark layout allows determining deformations in the same point, but on different directions.

By way of example, we used, for this paper, three test specimens of different polymeric composite materials. We noticed that for the elastic characteristics, both Young's modulus and Poisson's ratio, of single-layer reinforcement materials differed significantly from one stress direction to the next. Since tensometric mark measurements occur in the same point, the differences are caused only by the different stress directions. Finite element analysis revealed that the results of tensometric mark measurements are influenced neither by the stress device, nor by the metallic strengthening coating applied on the specimens in order to prevent their crushing upon stress application. The specific longitudinal and transverse deformation results are recorded by the Vishay P3 bridge, and the strain results are read on the testing equipment. Therefore, the number of points used for graph drawing may be rather high. Polymeric matrix composite materials have a viscous-plastic behaviour and hence the characteristics curves have a first nonlinear portion. In consideration of this last finding, we recommend that the approximation lines be drawn tangent to the  $\sigma$ - $\epsilon_L$  and  $\epsilon_T$ - $\epsilon_L$  curves in the area where the latter have a linear variation.

*Aknowlegment: This work has been supported by CNCSIS-Romania under the ID\_597/2007 project.*

## References

1. BĂRSĂNESCU, P.D., MOCANU F., BEJAN L., BĂTCĂ C., *Tensometrie electrică rezistivă la materialele compozite*, Ed. Tehnopress, Iași, 2007, p. 127
2. HWANG, S.F., YEH, C.K., CHUNG, S.C., *Inverse determination of elastic constants of composite materials*, *Polymer Composites*, **30**, Issue 5, 2009, p. 521
3. BOTELHO, E.C., SILVA, R.A., PARDINI, L.C., REZENDE, M.C., *A review on the development and properties of continuous fiber/epoxy/aluminum hybrid composites for aircraft structures*, *Mat. Res.*, **9** no.3, São Carlos, July/Sept. 2006
4. PENG, X.Q., CAO, J., *Numerical Determination of Mechanical Elastic Constants of Textile Composites*, 15th Annual Technical Conference of the American Society for Composite, College Station, TX, Sept. 2000, p. 25
5. LIAW, P.K., YU, N., HSU, D.K., MIRIYALA, N., SAINI, SNEAD, L.L., MCHARGUE, C.J., LOWDEN, R.A., *Modulus determination of continuous fiber ceramic composites*, *Journal of Nuclear Materials*, 219, 1995, p 93

---

Manuscript received: 19.05.2010